Solution to Stellarator Boundary Value Problems with a new Set of Simple Toroidal Harmonic Functions

W. Dommaschk

Max-Planck-Institut für Plasmaphysik, EURATOM Association

Z. Naturforsch. **36a**, 251–260 (1981); received January 21, 1981

Two types of 3D boundary value problems are solved for boundary conditions on a closed toroidal surface with axial or N-fold symmetry around the Z axis of a cylindrical coordinate system R, Φ, Z. In case I a surface current distribution is computed which generates inside the torus a given magnetic vacuum field. In case II a vacuum field within the torus with finite toroidal flux and zero surface normal is calculated. The method of solution is based on the availability of some complete set of auxiliary field harmonics which are regular outside the torus in case I and regular inside the torus in case II. The applied formalism is presented together with a new complete set of special field harmonics suited for case II and especially for the analytical representation of stellarator fields. The convergence of the solution method is tested and examples relating to stellarator field configurations are shown.

1. Introduction

The need for a solution to boundary value problems of the two types discussed in this paper has mainly arisen in connection with stellarator field optimization problems. The first type of problem (case I) arises if a given (analytical) field has to be generated by currents in a real device. The second type (case II) corresponds to, for example, the adaption of a field configuration to a predefined magnetic surface or to ideal fluid motion in a doubly connected spatial region of prescribed surface shape.

In both of the above mentioned cases the solution method to be presented assumes that: 1) a closed toroidal surface is given which is N-fold or axially symmetric around the Z axis of a cylindrical coordinate system R, Φ, Z, 2) some vacuum field is given for the region inside the torus, where it has to be nonsingular, 3) a complete auxiliary set of field harmonics is available.

In case I the scalar potential and its gradient must be explicitly available for all fields to be used. The functions of the auxiliary set must be regular and single-valued outside the torus with the exception that one of the auxiliary potentials may be multi-valued around the minor circumference of the torus. A linear combination from the auxiliary set is used to describe the field in the region outside the torus. The coefficient of the multi-valued potential is obviously determined in advance by the net toroidal surface current which has to be prescribed (see below). The residual coefficients are adjusted to get agreement at the surface between the normal components of the field outside and the field given inside the torus. The prescription of the normal components at the closed toroidal surface represents a well posed Neumann boundary value problem in the outer domain whose solution is unique since the net toroidal current is prescribed in addition. This current is equal to the value of the closed path integral over the magnetic field or to the corresponding increment of the scalar potential around the small circumference of the torus. Cases with zero net toroidal surface current correspond to the classical stellarator which has alternating currents around the minor torus circumference. A non-zero net toroidal current, on the other hand, corresponds to conditions in torsatrons if this current is properly chosen.

The surface current is determined by the difference between the surface tangent vectors of the fields outside and inside the torus and is shown to be divergenceless. The stream lines of the current density are shown to be the contour lines of the scalar potential difference between the two fields at the surface. The procedure determines a field distribution which is maintained by no other singularities than the surface currents and agrees inside the torus with the given field.

In case II only the field vector must be explicitly available for all fields to be used. The auxiliary set

Reprint requests to Frau Dr. L. Johannsen, Max-Planck-Institut für Plasmaphysik, EURATOM-Association, D-8046 Garching b. München.

0340-4811 / 81 / 0300-0251 $ 01.00/0. — Please order a reprint rather than making your own copy.

of functions (and the corresponding scalar potentials) must be regular and single-valued inside the torus. A linear combination from the auxiliary set is used in this region to describe a field which is then adjusted to compensate the surface normal components of the given field to zero. This again constitutes a Neumann boundary value problem. The resulting coefficients of the linear combination render a "Fourier decomposition" of the given field with respect to the applied auxiliary functions and to the prescribed toroidal surface. If the potential of the given field is single-valued with respect to the toroidal coordinate Φ, the resulting composite field (given field + linear combination) approaches zero. If, on the other hand, this field is especially chosen to be the field of a constant current along the Z axis (scalar potential proportional to Φ) then the resulting composite field is the solution to the problem of finding the field of which one magnetic surface coincides with a prescribed toroidal surface.

2. Formalism

The formalism presented in this section is valid for both of the above mentioned cases if not otherwise stated. Let $\boldsymbol{B} = \boldsymbol{B}(R, \Phi, Z)$ be the vector of the field to be given (the absolute value is denoted by B) for the region inside the torus, $\boldsymbol{F}_j = \boldsymbol{F}_j(R, \Phi, Z)$ the vector of the j-th auxiliary field function and C_j its (scalar) coefficient in the linear combination (where $j = 1, 2, \ldots, J$), $\boldsymbol{n} = \boldsymbol{n}(R, \Phi, Z)$ the unit surface normal vector (if R, Φ, Z is a point at the surface), and df the scalar element of surface. For the time being the net toroidal current is taken to be zero. The non-zero case is discussed below. In the index range j (or i) $= 1, 2, \ldots, J$ the vector functions $\boldsymbol{F}_j$ and corresponding scalar potentials are assumed to be single-valued throughout this paper. Also throughout this paper a normalization is assumed such that one chooses as the unit of length a value near the major radius of the torus and as the unit of the magnetic field the main field at the (normalized) radius $R = 1$ (which corresponds to the accepted unit of length). In this normalization the main field is thus always given by $\boldsymbol{B} = (0, 1/R, 0)$, where the values in parentheses are the components of the field in cylindrical coordinates R, Φ, Z and, correspondingly, by the scalar potential $U = \Phi$. A homogeneous field in the direction of Z which is p times stronger than the main field at $R = 1$ is thus to be given by, for example, $\boldsymbol{B} = (0, 0, p)$ and by the scalar potential $U = pZ$.

The C_j are adjusted to minimize the surface integral:

$$\int \left(\left(\boldsymbol{B} \mp \sum_{j=1}^{J} C_j \boldsymbol{F}_j \right) \boldsymbol{n} \right)^2 G \, \mathrm{d}f . \tag{1}$$

Here $G = G(R, \Phi, Z) > 0$ is a scalar weighting function (usually put to 1). The upper sign corresponds to case I, the lower sign to case II. The minimization of (1) yields for the C_j the system of equations:

$$\sum_{j=1}^{J} A_{ij} C_j = R_i , \quad i = 1, 2, \ldots, J . \tag{2}$$

Here $A_{i,j}$ and R_i ($i, j = 1, 2, \ldots, J$) are defined by

$$A_{ij} = \int (\boldsymbol{F}_i \boldsymbol{n}) \cdot (\boldsymbol{F}_j \boldsymbol{n}) \, G \, \mathrm{d}f , \tag{3}$$

$$R_i = \pm \int (\boldsymbol{F}_i \boldsymbol{n}) \cdot (\boldsymbol{B} \boldsymbol{n}) \, G \, \mathrm{d}f . \tag{4}$$

After solving (2) the sum expression inside the innermost parentheses of (1) is explicitly known. In case I it represents an approximation to the field required outside the torus. In case II the whole expression inside the innermost parentheses of (1) represents the explicit approximation to the field required inside the torus.

In case I (upper sign in (1) and (4)) the stream lines of the surface current are determined as follows: Let U and V be the scalar potentials inside and outside the torus i.e.

$$\nabla U = \boldsymbol{B} , \tag{5}$$

$$\nabla V = \sum_{j=1}^{J} C_j \boldsymbol{F}_j . \tag{6}$$

Let 1 and 2 be two points at the torus surface. The amount I of current which flows between these points is determined by a closed path integral over the magnetic field from 1 to 2 inside and from 2 to 1 outside the torus. Because of (5, 6) this yields

$$I \propto U_2 - U_1 + V_1 - V_2 . \tag{7}$$

The subscripts in this equation denote points 1 and 2. If point 1 is kept fixed and point 2 moves, $I =$ const. determines the stream line:

$$U - V = \text{const.} \tag{8}$$

Situations in which the net toroidal current in case I (upper sign in (1) and (4)) is different from zero may be included by a slight change of (1, 4, 6). To do this, we extend the summation in (1) and (6)

from $j=1, 2, \ldots, J$ to $j=0, 1, 2, \ldots, J$. We assume the scalar potential of the new additional term $C_0 * \boldsymbol{F}_0$ to be multi-valued around the small circumference of the torus and define the scalar coefficient C_0 in advance to be equal to the net toroidal current (which has to be prescribed) divided by the scalar potential increment of $\boldsymbol{F}_0$ around the minor torus circumference. In (4) we replace $\boldsymbol{B}$ by $\boldsymbol{B} - C_0 * \boldsymbol{F}_0$. Equations (2, 3, 5, 7, 8) remain unchanged.

The divergence of the surface current density is zero. This is easily derived from (7) by assuming some arbitrary triangular figure (which can be contracted to a point) on the surface and with vertices 1, 2, 3. If the right sides of (7) are summed for the three sides of the figure then the result is seen to be zero.

3. Field Harmonics

As an auxiliary set of functions for the region outside the torus (case I) the well known toroidal field harmonics of the first kind are used, which are singular on the circle $R=1, Z=0$ (which must be enclosed by the toroidal surface) and regular everywhere else [1]. One factor in these functions is the half-order Legendre function $P^m_{l-1/2}(\cosh \mu)$ of the first kind where μ depends on R and Z. The residual factor is periodic with m periods in the toroidal and l periods in the poloidal direction. The numerical representation of the above Legendre functions requires some caution to avoid undue losses of accuracy. Good results were obtained with the following integral representation [2] whose integrand is non-negative:

$$P^m_\nu(x) = \gamma(m,\nu) \cdot (x^2-1)^{m/2} \cdot \int_0^\pi [x + (x^2-1)^{1/2} \cos(t)]^{\nu-m} \cdot \sin^{2m}(t)\, dt . \tag{9}$$

Here γ is a scale factor depending only on m and ν. The evaluation of the integral (and also its derivative with respect to x) was done by Gauss-Legendre integration of order greater than or equal to $2m$ and with $\mathrm{tg}(t/2)$ as the variable of integration.

As a possible auxiliary set of functions for the region inside the torus (case II) the toroidal field harmonics of the second kind could be used [1]. They are obtained by using the half-order Legendre functions of the second kind $Q^m_{l-1/2}(\cosh \mu)$ in place of $P^m_{l-1/2}(\cosh \mu)$ in the above mentioned field harmonics. Another equivalent set could be obtained with Bessel functions. Both systems of functions were used in [3] to represent stellarator field configurations and to calculate corresponding magnetic surfaces.

For the present work we used a different complete set of functions for the region inside the torus, which is described in [4]. This set was used not only as an auxiliary set for case II but also for the analytical representation of the prescribed interior field in case I. A short characterization of this set follows. It is supplemented in Appendix 1 (and in [4]). Interrelations to vector potentials and Bessel functions (not in [4]) are discussed in Appendix 2. The set contains up to 4 different types of elements. A characteristic linear combination which contains one element of each type (with coefficients a, b, c, d) is represented by the scalar potential:

$$\begin{aligned} V_{m,l}(R,\Phi,Z) = {} & (a\cos(m\Phi) + b\sin(m\Phi)) \cdot D_{m,l}(Z,R) \\ & + (c\cos(m\Phi) + d\sin(m\Phi)) \cdot N_{m,l-1}(Z,R) . \end{aligned} \tag{10}$$

Here $c=d=0$ is valid if $l=0$. The integer indices m and l have to be greater than or equal to zero and denote the toroidal and poloidal periodicity. The functions $D_{m,n}(Z,R)$ and $N_{m,n}(Z,R)$ are relatively simple, finite and non-separable expressions without singularities for $R>0$ and for finite values of R and Z and are obtained as solutions of the Laplace equation after separation of the toroidal angle. With respect to Z they are polynomials of degree n. Since $D_{0,0}=1$, $D_{0,1}=Z$ (see Appendix 1), it is not difficult to recognize some of the simplest fundamental fields in (10). The potential $U=Z$ of a vertical field of strength 1 (in the applied normalization) is obtained from, for example $V_{0,1}$ with $a=1$, $b=c=d=0$. The (normalized) potential $U=\Phi$ of the main field is obtained from $V_{m,0}$ with $a=c=d=0$, $b=1/m$ and $m->0$. This field is or may be regarded as a constituent of $\boldsymbol{B}$ in (1) and is therefore not used as an element $\boldsymbol{F}_j$ in the sum expression.

The functions $D_{m,n}$ and $N_{m,n}$ have the following property at $R=1$:

$$D_{m,n} = Z^n/n!, \quad \partial D_{m,n}/\partial R = 0, \tag{11}$$

$$N_{m,n} = 0, \quad \partial N_{m,n}/\partial R = Z^n/n!. \tag{12}$$

Fields produced by using $D_{m,n}(Z,R)$ are thus tangential at the cylindrical surface $R=1$ and can

satisfy Dirichlet-type boundary conditions there. Fields resulting from $N_{m,n}(Z, R)$ on the other hand are normal to this surface and can satisfy Neumann-type boundary conditions. Because of (11, 12) the expression (10) can be used to satisfy the following Cauchy-type boundary conditions at $R=1$:

$$V_{m,l} = (a\cos(m\Phi) + b\sin(m\Phi)) \cdot Z^l/l!\,, \tag{13}$$

$$\partial V_{m,l}/\partial R = (c\cos(m\Phi) + d\sin(m\Phi)) \cdot Z^{l-1}/(l-1)!\,. \tag{14}$$

This property shows that the set (10) is complete in the sense that every vacuum field which is non-singular in a toroidal region near $R=1$, $Z=0$, is periodic in Φ in the form of a truncated Fourier series up to and including the harmonic number M and is a polynomial of degree $L-1$ in Z at $R=1$ can be exactly represented by a linear combination of expressions (10) with m less than or equal to M and l less than or equal to L. This is the case because: 1) two vacuum fields are identical in space if they satisfy the same Cauchy boundary conditions at some surface. 2) at the surface $R=1$ the conditions (13, 14) can be made to agree for both fields term by term for every Fourier component and every power of Z by a proper choice of a to d in each of the $V_{m,l}$ in the linear combination.

The relation of (10) to stellarator fields is seen from the following. Let us take a linear combination of only one of the expressions (10) with the normalized potential $U=\Phi$ of the main toroidal field and choose $a=d=0$, $d=\pm b$. This yields a stellarator field configuration in the toroidal region near $R=1$, $Z=0$ with m toroidal and l poloidal field periods and with a circular magnetic axis if $l>1$. For $l>0$ the configuration is qualitatively equivalent to the interior field produced by helical currents flowing around a circular torus with a rotational transform m/l of the stream lines on the torus. A left-handed screw is produced if $d/b=(-1)^{**}l$, a right screw for the other sign of d/b, and for $l=2$ the rotational transform t of the magnetic field lines near the magnetic axis relates to b by

$$|b| = (t(m-t))^{1/2}, \quad t \leq m/2\,. \tag{15}$$

Here a change in the sign of b corresponds to a toroidal phase shift by half of the toroidal period.

4. Evaluation

The form of the toroidal surface is defined by

$$R = R_0(\Phi) + S\,R_1(\Phi, \vartheta)\,, \tag{16}$$

$$Z = Z_0(\Phi) + S\,Z_1(\Phi, \vartheta)\,. \tag{17}$$

Here R, Φ, Z are the coordinates of a point at the surface, R_0, R_1, Z_0, Z_1 are periodic functions of the poloidal angle $\vartheta = \operatorname{arctg}(Z-Z_0)/(R-R_0))$ and/or the toroidal angle Φ. S is a constant which determines an aspect ratio. The choice of the right-hand sides of (16, 17) is quite unrestricted with the exception that in case I the singularities of the auxiliary field harmonics must lie inside the surface. The right sides of (16, 17) must be supplied (in analytical form) together with their partial derivatives with respect to Φ and ϑ. The derivatives are needed to compute the surface normal vector $\boldsymbol{n}$ and the functional determinant relating $\mathrm{d}\Phi^*\mathrm{d}\vartheta$ to df in surface integrals.

The surface integration is done by discretization and Fourier summation in the variables Φ and ϑ. The necessary refinement of this discretization is governed by some maximum tolerable deviation of the integrand in the surface integral (1) from zero. As a measure for this error we use

$$\varepsilon = \frac{\left|\left(\boldsymbol{B} \mp \sum_{j=1}^{J} C_j \boldsymbol{F}_j\right)\cdot \boldsymbol{n}\right|_{\max}}{(|\boldsymbol{B}\cdot\boldsymbol{n}|_{\max} + e\langle B\rangle)}\,. \tag{18}$$

The maxima in the numerator and denominator are independently taken from the set of all discretization points as the surface and may thus belong to different points. The term $e\langle B\rangle$ (where $\langle B\rangle$ is an average of B and e a constant of the order of the mashine accuracy) avoids division by zero in singular cases. In order that (18) makes sense and to get reasonable results, the number of discretization intervals must not fall short of some lower limit. This limit is found from the requirement that at least a rough representation by discretization must be possible in principle for each of the J field harmonics applied in (1, 6). Since a fourth-order polynomial (5 constants) is at least necessary to represent the full period of a wave there should be at least 4 discretization intervals available along the distance of the shortest oscillation interval which might be produced by one of these field harmonics. Let the whole configuration (boundary conditions + field) have N-fold symmetry around the axis Z.

Then toroidal harmonic numbers $m = k*N$, with $k = 0, 1, 2, \ldots$ and poloidal harmonic numbers $l = 0, 1, 2, \ldots$ may be present in the field. If only field harmonics $\boldsymbol{F}_j$ with $k \leqq K$ (i.e. $m \leqq K*N$) and $l \leqq L$ are admitted in (1, 6), then $N_t = 4K$ and $N_p = 4L$ discretization intervals, respectively, should at least be used for one toroidal field period ($1/N$ of the full angle) and for the full poloidal angle, respectively.

The appropriate choice of K and L depends on the convergence of the sum expression in (1, 6) in the special problem under consideration. If the surface is axially symmetric then there is no coupling of different toroidal harmonics via the boundary conditions. In this case K needs not to be larger than the largest k of toroidal Fourier harmonics considered as relevant in $\boldsymbol{B}$. This is not the case if the surface has a weaker symmetry and a similar statement is not necessarily true of L in any case even if the small torus cross-section is circular.

The number J of field harmonics which are actually needed in (1, 6) for given values of K and L is reduced by symmetry properties of the configuration and by the fact that the surface integral of the normal component of the magnetic field must be zero. If besides the N-fold symmetry there is no further symmetry (case S1), one has $J = 2*(2K*L + K + L)$. The above value of J is halved if a further symmetry is present with the property that the transformation $\Phi \to -\Phi$, $Z \to -Z$ reflects the toroidal surface into itself and U in (5) into $+U$ (case S2) or $-U$ (case S3). The radial component of ∇U then changes its sign as U, the other components changing sign if U does not and vice versa under this transformation. The reduction of J in cases S2 and S3 occurs because the special symmetry of the surface imprints the symmetry of U on V in (6) via the boundary conditions.

5. Results

Computations for both of the above mentioned types of boundary value problems denoted as cases I and II (Sect. 1) have been carried out mainly for configurations with 10-fold symmetry around the Z axis. This has been done up to now for the above mentioned symmetry type denoted as case S3 (Sect. 4) for 10-fold symmetric fields and axial symmetric boundary conditions as well as for configurations where the fields as well as the toroidal surface were 10-fold symmetric. With $J < 50$ the best results with an error parameter (18) of $\varepsilon < 0.005$ were obtained for axially symmetric toroidal surfaces with circular minor cross-sections for an aspect ratio $A = \langle R \rangle / \langle r \rangle$ not less than 5 (where $\langle R \rangle$ and $\langle r \rangle$ denote mean values of the major and minor torus radius, respectively). Surfaces of weaker symmetry required larger values of A to get comparable errors even for $50 < J < 150$. This was observed in case I even if the singularity of the auxiliary field was sufficiently centered inside the torus as well as in case II where no such singularity is present. Apart from the requirement for the singularity the results seem to indicate as an additional requirement for both cases I and II that the toroidal curvature of the surface must be sufficiently small everywhere against its poloidal curvature in order to get a sufficient convergence of (6).

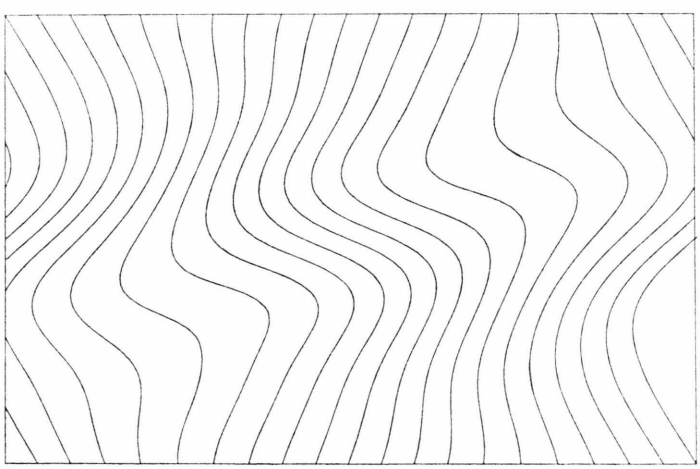

Fig. 1. Example of case I. Projection of stream lines on a 10-fold symmetric toroidal surface into the plane of the toroidal angle (abscissa, (1/10 of the full angle) and the poloidal angle (ordinate, full angle from torus outside to outside).

In Fig. 1 a solution to case I is shown where the given field is the analytical stellarator field configuration discussed in [5] (loc. cit. Fig. 1, column 1). This configuration has $N=10$ periods and contains partial fields with $l=1$ and 2. The picture shows stream lines (with a constant amount of current between neighbouring lines) on a toroidal surface in the plane of the toroidal angle Φ (abscissa, $1/N$ of the full angle) and the poloidal angle ϑ (ordinate, full angle, from outer torus aequator). The surface (16, 17) was described in this case by

$$R_0 = 1 + 0.01 \cos(10\Phi),$$
$$Z_0 = 0.015 \sin(10\Phi), \quad S = 1/A,$$
$$H = S(1 - 0.05 \cos(2\vartheta)),$$
$$R_1 = H \cos(\vartheta), \quad Z_1 = H \sin(\vartheta),$$

where $A=11$ was chosen for the aspect ratio and $\langle R\rangle = 1$ as the mean value of the major radius. The surface corresponds to a 10-fold symmetric toroid with respect to the Z axis with a non-circular minor cross-section whose position in the R, Z plane depends on its position in the toroidal direction. The calculation was done with $K=L=8$, $J=144$, $N_t = N_p = 60$ and the resulting error (18) was $\varepsilon = 0.0057$. An improved symmetry of the above surface (pictures not shown) reduced this error by one order of magnitude if the minor cross-section of the surface was made circular ($H=S$), by 1.2 orders of magnitude if the surface was made axially symmetric ($R_0=1$, $Z_0=0$) and by 3.1 orders of magnitude if both simplifications of the surface were applied at the same time. In the last two cases the number of auxiliary functions could, moreover, be reduced to $J=42$ (with $K=2$, $L=8$) because of the axial symmetry for reasons discussed near the end of Section 4.

Figures 2a to c show cross-sections of magnetic surfaces* in three different meridian planes (1/4 of a toroidal field period apart from each other). These magnetic surfaces belong to a 10-fold symmetric field configuration which was obtained as the result of a solution to case II, where one of the surfaces and $U=\Phi$ in (5) were prescribed. In (16, 17) this surface was defined by:

$$R_0 = 1 + 0.02 \cos(10\Phi),$$
$$Z_0 = 0.02 \sin(10\Phi), \quad S = 1/A,$$

* The representation of the calculated configurations as shown in Figs. 2 and 5 was obtained with a program of W. Lotz.

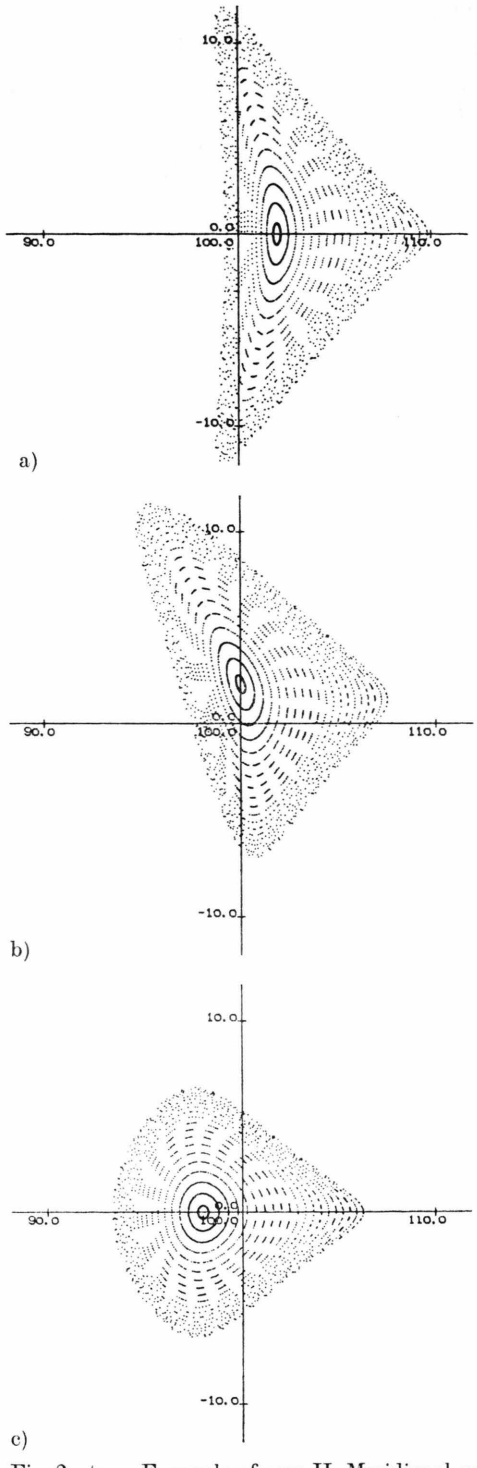

Fig. 2a to c. Example of case II. Meridional cross-sections of 10-fold symmetric toroidal magnetic surfaces as obtained from a field configuration which was found by prescribing one of the innermost surfaces. The toroidal distance of pictures a to c is 1/4 of a period.

$$H = S(1 - 0.28(\cos(2\vartheta - 10\Phi) + \cos(2\vartheta)))\,,$$
$$R_1 = H\cos(\vartheta)\,,\quad Z_1 = H\sin(\vartheta)\,,$$

This corresponds to a surface of 10-fold symmetry with respect to the Z axis with a minor cross-section whose position, form and direction depend on Φ, as may be seen from Figs. 2 (where 100 means 1) for large aspect ratios. The solution of the boundary value problem was done with $A = 1000$, $K = 2$, $L = 3$, $J = 17$, $Nt = N_p = 30$ and led to an error $\varepsilon = 0.006$. As can be seen, the resulting field configuration has smooth magnetic surfaces for A not less than about 20. Apart from a few exceptions (see Figs. 4 and 5) case II has been investigated up to now only with the relatively small values of K and L given above. The existence of smooth surfaces still far beyond the prescribed one was observed in most of these cases if the aspect ratio of the prescribed surface was sufficiently large. On the other hand, poor convergence and large error parameters were obtained in all of these cases if it was attempted to prescribe a non-trivial (not axially symmetric) surface and to use a moderate value of A from the beginning. This indicates that the analytical form of magnetic surfaces for field configurations (6) and for small values of A and J is quite restricted.

Figures 3 and 4 exemplify the dependence of the error (18) on different parameters of the surface for some typical cases of special interest. Figure 3 shows results obtained for case I with the same field configuration which was used for Fig. 1. The surface (16, 17) was defined by

$$R_0 = 1 + g\cos(10\Phi)\,,\quad Z_0 = g\sin(10\Phi)\,,$$
$$R_1 = S\cos(\vartheta)\,,\quad Z_1 = S\sin(\vartheta)\,,\quad S = 1/A\,.$$

With a constant aspect ratio $A = 11$. The picture shows the dependence of ε on the amplitude g (which is a measure of the deviation of the surface from axial symmetry) and on the number J of auxiliary field harmonics applied in (1, 6). The computations were done with $K = L$ and a relatively large number of surface points ($N_t = N_p \approx 7.5 * K$) as compared to the above given lower limit (Section 4). As can be seen from the figure, the error may become extremely small for weak deviations from axial symmetry of the surface, but it is difficult to get reasonably small errors for larger deviations from the axially symmetric case even with a large number J of auxiliary functions.

Figure 4 shows a result obtained for case II. The surface (16, 17) was defined by

$$R_0 = 1\,,\quad Z_0 = 0\,,$$
$$H = S/(1.67\cos^2(u) + 0.60\sin^2(u))^{1/2}\,,$$
$$S = 1/A\,,\quad u = \vartheta - 5\Phi\,,\quad R_1 = H\cos(\vartheta)\,,$$
$$Z_1 = H\sin(\vartheta)\,.$$

The surface is 10-fold symmetric with respect to the Z axis, and its minor cross-section is an ellipse centered at $R = 1$, $Z = 0$ with a constant ratio 0.6 of its half-axes, whose geometric mean equals S. The orientation of the ellipse depends on Φ and changes by 180 degrees (transforms into itself) if Φ

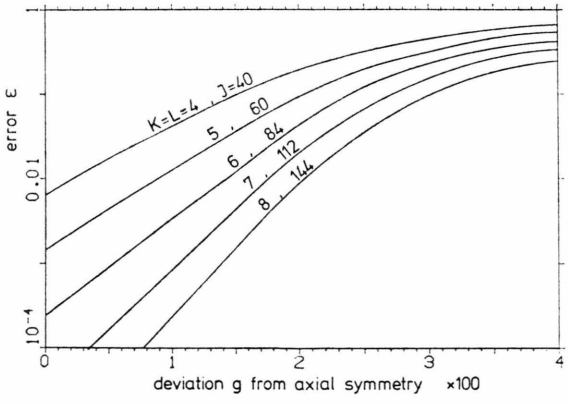

Fig. 3. Example of case I. Dependence of the error ε (Eq. (18)) on the deviation of a 10-fold symmetric surface from axial symmetry (abscissa) and on the number J of auxiliary fields admitted for the calculation.

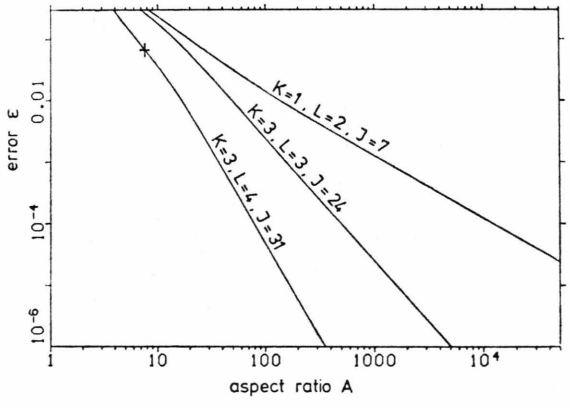

Fig. 4. Example of case II. Dependence of the error ε (Eq. (18)) on the aspect ratio (abscissa) of a prescribed 10-fold symmetric toroidal magnetic surface and on different combinations of auxiliary fields admitted for the calculation.

changes by 36 degrees. The content of Fig. 4 is in agreement with the above comments to Figures 2. For small values of the aspect ratio A and small values of J the convergence of (6) becomes unsatisfactory. For larger values of A, however, it is easy to get a small error parameter even with a relatively small number J of auxiliary functions. The same would be the case for smaller values of A if the deviation of the surface from axial symmetry were smaller than in the given example, which is somewhat critical.

Figures 5a to c show magnetic surfaces and refer to the case indicated in Fig. 4 by a cross at $A = 7.8$ and $\varepsilon = 0.065$. The representation is the same as was described for Figure 2. The example shows that quite reasonable solutions to case II may be found with an increased number J of auxiliary fields even for relatively small aspect ratios of the prescribed surface and in spite of the relatively large error parameters resulting. In contrast to cases where the aspect ratio of the prescribed surface was very large, as in Fig. 2, the surfaces of Fig. 5 cease to exist almost immediately outside the prescribed one. This situation might possibly be changed by a more refined calculation with the same small value of ε that was obtained in the case of Figure 2.

6. Conclusion

3 D boundary value problems of relevance for stellarators have been solved for boundary conditions on toroidal surfaces for two types of boundary conditions (cases I and II above). A new complete set of field harmonics for the interior of the torus has proved useful here because each of these fields is a relatively simply structured finite expression which represents a typical stellarator field with a unique toroidal and poloidal periodicity. Within the limitations mentioned in Sect. 5 the described method has proved useful in case I because if finds the shape and position of the continuous analogue of the so called Wobig Rehker coils [6, 7]. As a further application, currently being in progress, discrete Wobig Rehker coils may be obtained by discretization of the calculated current distribution. Calculations made for case II have also proved of advantage since, for example, the field configurations discussed in [5] (loc. cit. Fig. 1) were generated by optimization of configurations which were originally obtained by prescribing the shape of magnetic surfaces.

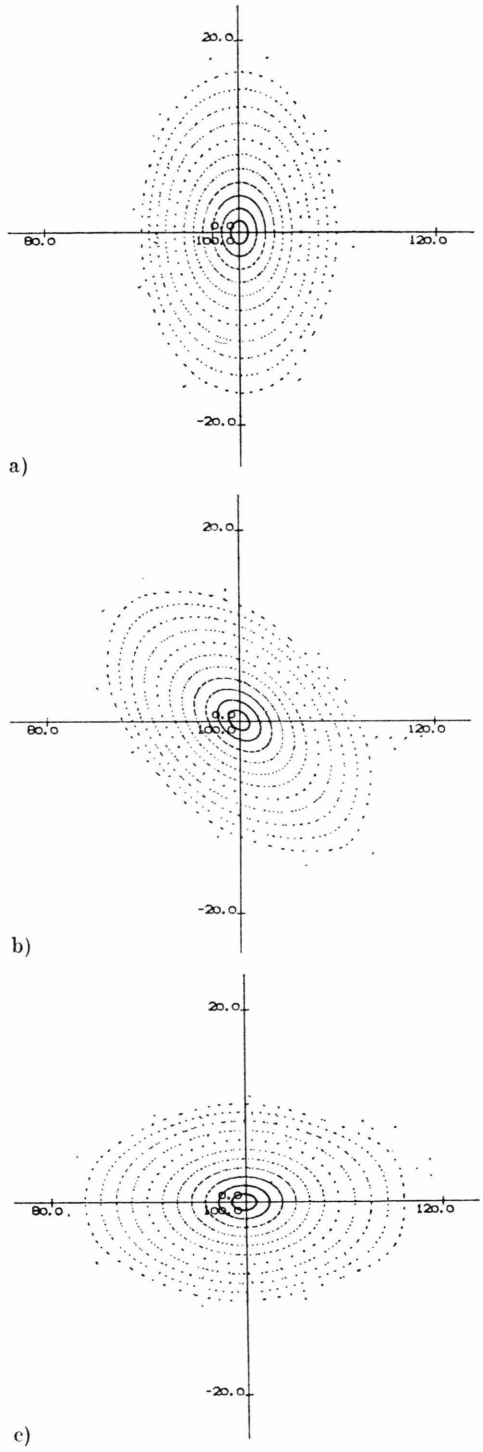

Fig. 5a to c. Example of case II. Meridional cross-sections of a 10-fold symmetric helical $l = 2$ configuration where one of the outermost magnetic surfaces (with aspect ratio 7.8) was prescribed. The toroidal distance of pictures a to c is 1/4 of a period.

Acknowledgements

The author would like to thank A. Schlüter for his continuous interest as well as for useful discussions and J. Nührenberg for his stimulating advice and critical comments. He is also indebted to W. Lotz for his support of the present work by his program for calculating magnetic surfaces and for critical remarks.

7. Appendix 1

The functions $D_{m,n}(Z, R)$ and $N_{m,n}(Z, R)$ in (10) are found in [4] (in a slightly different notation) as follows. Let

$$U = f(Z, R)\exp(\pm i m \Phi),$$
$$m = 0, 1, 2, \ldots, \tag{A.1}$$

be required to solve the Laplace equation $\Delta U = 0$ in cylindrical coordinates R, Φ, Z, where $f(Z, R)$ is assumed to be independent of Φ and i is the imaginary unit. Then $f(Z, R)$ is found to satisfy this equation if $f = \mathrm{I}_{m,n}(Z, R)$ and

$$I_{m,n}(Z, R) = \sum_{k=0}^{2k \leq n} \frac{Z^{n-2k}}{(n-2k)!} C_{m,k}(R),$$
$$n = 0, 1, 2, \ldots. \tag{A.2}$$

Here n is a non-negative integer and the summation** proceeds down to the lowest possible non-negative power of Z. The functions $C_{m,k}(R)$ in this expression are independent of Φ and Z and defined recursively by

$$C_{m,k}(R) = \frac{1}{2m}\int_1^R C_{m,k-1}(s)\cdot((s/R)^m - (R/s)^m)\, s\, \mathrm{d}s, \quad \text{if} \quad m > 0, \tag{A.3}$$

$$C_{0,k}(R) = \int_1^R C_{0,k-1}(s)\cdot(\ln(s) - \ln(R))\, s\, \mathrm{d}s, \quad \text{if} \quad m = 0. \tag{A.4}$$

The recursion is started in two alternative ways which yield two different possible types of functions $I_{m,n}$ for each pair of indices m and n. These functions (which are linearly independent of each other) are given the above notations $D_{m,n}(Z, R)$ and $N_{m,n}(Z, R)$. For $D_{m,n}$ the recursion starts with:

$$C_{m,0}(R) = (R^m + R^{-m})/2, \quad \text{if} \quad m > 0, \tag{A.5}$$
$$C_{0,0}(R) = 1, \quad \text{if} \quad m = 0. \tag{A.6}$$

For $N_{m,n}$ the recursion starts with

$$C_{m,0}(R) = (R^m - R^{-m})/2m, \quad \text{if} \quad m > 0, \tag{A.7}$$
$$C_{0,0}(R) = \ln(R), \quad \text{if} \quad m = 0. \tag{A.8}$$

The resulting sequences of expressions for $D_{m,n}$ and $N_{m,n}$ are thus found to begin with

$$D_{0,0} = 1, \quad D_{0,1} = Z,$$
$$D_{0,2} = Z^2/2 + (1 - R^2 + 2\ln(R))/4, \tag{A.9}$$
$$\ldots$$
$$D_{m,0} = (R^m + R^{-m})/2, \quad m = 1, 2, \ldots,$$
$$D_{m,1} = Z(R^m + R^{-m})/2, \quad m = 1, 2, \ldots,$$

$$D_{m,2} = Z^2(R^m + R^{-m})/4 + \{R^m[m(1-m)R^2 + (m+1)(m-2)] + R^{-m}[m(1+m)R^2 - (m-1)\cdot(m+2)]\}/(8m(m^2-1)),$$
$$m = 2, 3, \ldots,$$
$$D_{1,2} = Z^2(R + 1/R)/4 - (R^3 + 4R\ln(R) - 4R + 3/R)/16,$$
$$m = 1,$$
$$\ldots$$
$$N_{0,0} = \ln(R), \quad N_{0,1} = Z\ln(R),$$
$$\ldots$$
$$N_{m,0} = (R^m - R^{-m})/2m, \quad m = 1, 2, \ldots,$$
$$N_{m,1} = Z(R^m - R^{-m})/2m, \quad m = 1, 2, \ldots,$$
$$\ldots$$

Further details may be found in [4]. This mainly concerns formulas for the functions $C_{m,k}$ as obtained with REDUCE and FORTRAN routines with formulas for field components for all m and $l < 6$.

8. Appendix 2

The functions in Appendix 1 may be interrelated to vector potentials and to Bessel functions as follows.

8.1. Connection with Vector Potentials

With $D_{m,n}$ and $N_{m,n}$ the scalar potential $V_{m,l}$ (R, Φ, Z) is constructed with the aid of (10). Start-

** The use of the symbols C, k, in Appendix 1 and A, C, J, Z in Appendix 2 differs from their use in the main text.

ing from $V_{m,l}$, it is not difficult to get expressions for a two-component vector potential $A_{ml,} = A_{m,1}(R, \Phi, Z)$ whose toroidal component is zero and where

$$\boldsymbol{A}_{m,l} = (A_r, 0, A_z), \tag{A.10}$$

$$\nabla \times \boldsymbol{A}_{m,l} = (B_r, B_\varphi, B_z) = \nabla V_{m,l}. \tag{A.11}$$

Here A_r, A_z and B_r, B_φ, B_z denote components of the vector potential and the field adjoined to the scalar potential $V_{m,l}$. The indices m, l of these components have been omitted here for simplicity. Excluding fields with a multi-valued scalar potential such as the main field (where $A_r = 0$, $A_\varphi = 0$, $A_z = -\ln(R)$ is appropriate), (A.10) and (A.11) then lead to

$$A_r = -B_z(R, \Phi - \pi/2m, Z)\, R/m, \quad m = 1, 2, \ldots, \tag{A.12}$$

$$A_r = -B_z(R, 0, Z)\, \Phi R, \quad m = 0; \tag{A.13}$$

$$A_z = B_r(R, \Phi - \pi/2m, Z)\, R/m, \quad m = 1, 2, \ldots, \tag{A.14}$$

$$A_z = B_r(R, 0, Z)\, \Phi R, \quad \boldsymbol{m = 0}. \tag{A.15}$$

8.2. Connection with Bessel Functions

An interrelation between Bessel functions and the $C_{m,k}$ may easily be established. Multiplication of $I_{m,n}$ in (A.2) by $\exp(im\Phi)$ and by the n-th power of q (where q is a real or complex constant) and summation over n from zero to infinity yields a solution of the Laplace equation which separates (within some range of convergence) into a product of $\exp(im\Phi)$, $\exp(qZ)$ and a factor Z_m which depends only on m, q and R:

$$Z_m(q, R) = \sum_{k=0}^{\infty} q^{2k} C_{m,k}(R). \tag{A.16}$$

The series rapidly converges for sufficiently small absolute values of q and $R-1$ since in an expansion of the $C_{m,k}$ with respect to powers of $R-1$ the leading powers increase with k. Two different types of Z_m are obtained from (A.16), depending on whether $D_{m,n}$ or $N_{m,n}$ is used in place of $I_{m,n}$, i.e. whether (A.5) and (A.6) or (A.7) and (A.8) are used to determine the $C_{m,k}(R)$. A corresponding distinction is made below by using superscripts D or N. A comparison of the above solution of the Laplace equation with the well known Bessel function representation of field harmonics shows Z_m to be a cylinder function, i.e. a linear combination of two independent m-th order Bessel functions whose argument must be qR, and whose coefficients may depend on q. The coefficients are determined by the use of (11, 12) or by using the fact that $C_{m,0}(R) = 1$ for $R = 1$ if the recursion for $D_{m,n}$ is used and $C_{m,k}(1) = 1$ (where $'$) denotes the derivative with respect to R) if the recursion for $N_{m,n}$ is used and that all other $C_{m,k}$ and $C_{m,k}$ yield zero for $R = 1$. The result that the right side of (A.16) is a cylinder function could as well have been obtained from a hierarchy of differential equations for the $C_{m,k}$ as obtained in [4] (loc. cit. Equations 14). A simple manipulation of these equations leads to an equation for Z_m (if the series (A.16) converges sufficiently) which, in fact, proves to be the differential equation for cylinder functions with argument qR.

If one decides to use the two Bessel functions $J_{m,n}(qR)$ and $Y_{m,n}(qR)$ (whose Wronskian is $2/\pi q$) in the linear combination for Z_m the above considerations then lead to

$$J_m(qR) = J_m(q) Z_m^D(q, R) + qJ'_m(q) Z_m^N(q, R), \tag{A.17}$$

$$Y_m(qR) = Y_m(q) Z_m^D(q, R) + qY'_m(q) Z_m^N(q, R). \tag{A.18}$$

Here $'$) denotes the derivative with respect to the argument and the superscripts have the meaning stated above. A corresponding representation for Hankel functions is straightforward. Equations (A.17), (A.18) may be rewritten to show the expressions for both types of Z_m in terms of Bessel functions. These expressions may be looked at as the generating functions for the $C_{m,k}$. The $C_{m,k}$ are thus seen to be the coefficients of a power series development (with respect to the square of q) of certain types of cylinder functions.

[1] P. Morse and H. Feshbach, Methods of Theoretical Physics. McGraw-Hill, New York **1953**, pp. 1362.
[2] W. Magnus, F. Oberhettinger, and R. P. Soni, Formulas and Theorems for the Special Functions of Mathematical Physics, Springer-Verlag, Berlin **1966**, pp. 184.
[3] R. P. Freis, C. W. Hartman, J. Killeen, A. A. Mirin, and M. F. Uman, Nucl. Fusion **172**, 281 (1977).
[4] W. Dommaschk, IPP Report 0/38 (1978).
[5] R. Chodura, W. Dommaschk, W. Lotz, J. Nührenberg, A. Schlüter, R. Gruber, F. Herrnegger, W. Kerner, W. Schneider, and F. Troyon, IAEA-CN-38/BB2 1980.
[6] H. Wobig and S. Rehker, VII Symp. on Fusion Techn., Grenoble **1972**, p. 345.
[7] S. Rehker and H. Wobig, IPP Report 2/215 (1973).